Title:

Virtual Histology Analysis of Carotid Atherosclerotic Plaque:

Plaque Composition at the Minimum Lumen Site and of the Entire Carotid Plaque.

Authors:

Arihito Tsurumi, MD, PhD[1]; Yuko Tsurumi, MD[2]; Osamu Hososhima, MD[3]; Noriaki Matsubara, MD, PhD[4]; Takashi Izumi, MD, PhD[4]; Shigeru Miyachi, MD, PhD[4]

Affiliation:
1. Department of Neurosurgery, National Hospital Organization Nagoya Medical Center, Nagoya, Japan.
2. Department of Neurosurgery, Japanese Red Cross Nagoya Daiichi Hospital, Nagoya, Japan
3. Department of Neurosurgery, Tosei General Hospital, Seto, Japan
4. Department of Neurosurgery, Nagoya University Graduate School of Medicine, Nagoya, Japan

Correspondence to: Arihito Tsurumi, MD, PhD.
Department of Neurosurgery, National Hospital Organization Nagoya Medical Center,
4-1-1 San-no-maru, Nakaku, Nagoya 460-0001, Japan.
Phone: +81-52-951-1111
Fax: +81-52-951-0664
email: tsurumi@med.nagoya-u.ac.jp

Funding sources: none

Running Title: Virtual Histology analysis of carotid atherosclerotic plaque

Key words: carotid stenosis; plaque imaging; IVUS; Virtual Histology

This is the pre-peer reviewed version of the following article: [Tsurumi A, Tsurumi Y, Hososhima O, Matsubara N, Izumi T, Miyachi S. Virtual Histology Analysis of Carotid Atherosclerotic Plaque: Plaque Composition at the Minimum Lumen Site and of the Entire Carotid Plaque. J Neuroimaging. in press.], which has been published in final form at [Link to final article].

Virtual Histology Analysis of Carotid Atherosclerotic Plaque:
Plaque Composition at the Minimum Lumen Site and of the Entire Carotid Plaque.

Abstract

Background and Purpose. Virtual Histology intravascular ultrasound, which is based on spectral and amplitude analyses of the intravascular ultrasound radiofrequency backscatter signals, allows reliable identification of four atherosclerotic plaque types: fibrous, fibrofatty, dense calcium, and necrotic core. To detect the relationship between the volumetric analysis of the entire plaque responsible for carotid artery stenosis and cross-sectional plaque analysis at the minimum lumen site, a retrospective, cross-sectional study of patients who underwent interventional therapy of atherosclerotic cervical carotid artery stenosis was conducted.

Methods. Forty-eight stenotic lesions in 45 consecutive patients were included in the study. Virtual Histology was obtained before predilatation for the carotid artery stenting procedure.

Results. Simple regression analysis revealed that the volumetric proportion of each plaque type correlated significantly with the corresponding plaque type area at the minimum lumen site. The adjusted coefficients of determination of the simple regression analyses were 0.782 ($P < 0.001$) for fibrous tissue, 0.741 ($P < 0.001$) for fibrofatty tissue, 0.864 ($P < 0.001$) for dense calcium, and 0.918 ($P < 0.001$) for necrotic core.

Conclusions. The plaque composition at the minimum lumen site represents the volumetric composition of the entire carotid plaque that causes atherosclerotic cervical carotid artery stenosis.

Introduction

For the treatment of patients with carotid artery stenosis, plaque imaging to analyze plaque characteristics is important to detect vulnerable plaque and avoid ischemic complications. Magnetic resonance imaging,[1-4] computed tomography, [5,6] positron emission tomography,[7,8] carotid ultrasonography,[2] and intravascular ultrasound (IVUS)[9,10] have been reported as carotid plaque imaging devices. Several studies of coronary[11-13] and carotid[14] artery plaque imaging have demonstrated that Virtual Histology (VH; Volcano Corporation, Rancho Cordova, CA), which is based on spectral and amplitude analyses of the intravascular ultrasound radiofrequency backscatter signals, allows reliable identification of four atherosclerotic plaque types: fibrous, fibrofatty, dense calcium, and necrotic core. In addition, the geometric and compositional output of VH IVUS has been reported to be reproducible.[15] Therefore, VH IVUS has been used to evaluate plaque characteristics in both coronary interventions[16,17] and neurointerventions. [18-22]

The authors have previously reported that periprocedural hypotension in carotid artery stenting can be predicted by volumetric VH IVUS analysis of the plaque responsible for the carotid artery stenosis.[23] Volumetric analysis of the plaque, which can be achieved by performing integral analysis of the cross-sectional plaque analyses, is a time-consuming task. On the other hand, analyzing only one cross-section at the minimum lumen site is easier and faster than volumetric analysis.

The present study was conducted to identify the relationship between the volumetric analysis of the entire carotid plaque and cross-sectional plaque analysis at the minimum lumen site.

Methods

Study Design

A retrospective, cross-sectional study of patients who underwent interventional therapy to cervical carotid artery stenosis in a tertiary referral hospital from April 1, 2006 to April 30, 2007 was conducted. The VH IVUS data and demographic characteristics of each patient were gathered and recorded for the purpose of analyzing the relationship between the clinical prognosis in carotid artery stenting (CAS) and carotid plaque characteristics, which had been reported in our previous paper. All consecutive patients who underwent interventional therapy for cervical carotid artery stenosis in our hospital were registered and recorded in the present study. Patients with stenosis related to radiation therapy or with restenoses after carotid endarterectomy (CEA) were excluded from the present study. All patients underwent VH IVUS and volumetric and cross-sectional analyses of the carotid plaque. The patients who had stenosis that was too severe for the VH IVUS catheter to cross before predilatation for CAS were also excluded from the study.

Virtual Histology Acquisition

All procedures were performed under local anesthesia. A VH IVUS was obtained before predilatation for the CAS procedure. A VH IVUS catheter (Eagle Eye Gold, 3.5 F/20 MHz; Volcano Corporation) was placed distal to the stenotic lesion and manually pulled back proximal to the stenosis. During this pullback, color flow IVUS was recorded on the VH IVUS console. Then, the VH IVUS catheter was again advanced distal to the stenosis, and it was subsequently pulled back proximal to the stenosis by a motorized pullback system set at 0.5 mm/sec. During this pullback, raw radiofrequency data were captured on the VH IVUS console at the top of the R-wave of the electrocardiogram and recorded on a digital video disc. Each distance between the captured images was also recorded.

Analysis of Virtual Histology

The color-coded map superimposed on the gray-scale IVUS tomographic image was reconstructed from the captured raw RF data using the VH IVUS software (version 1.3; Volcano Corporation). Using the VH IVUS software, atherosclerotic plaques were characterized by classification trees based on mathematical autoregressive spectral analysis of IVUS backscattered data. The distal/proximal end frames were defined as the frames where the plaque within the media line was concentric and the diameter of the lumen within the intima did not change compared with more distal/proximal frames. Between the distal and proximal end frames, a media line and an intima line were manually drawn in each frame by referring to the adjacent frames and by referring to the corresponding color flow IVUS image, respectively. Referring to adjacent frames is useful in detecting the media line. The intima line can be detected easily using the color flow IVUS images showing the blood flow in the vessel. Since the VH IVUS software could not analyze the plaque within ulceration, the ulcerated area was considered to be within the intima line in VH IVUS analyses.

The total volume of each plaque type (fibrous, fibrofatty, dense calcium, and necrotic core) was calculated using the VH IVUS software and expressed in cubic millimeters. The volumetric proportion of each plaque type was also determined. The square measure of each plaque type at the minimum lumen site, which was determined as the point of minimum lumen

size, was also calculated using the VH IVUS software and expressed in square millimeters. The proportion of the area of each plaque type at the minimum lumen site was also determined.

Statistical Analysis

A simple regression analysis was performed to examine the effects of the proportion of the four plaque types at the minimum lumen site on the volumetric proportion of each plaque type. A P value < 0.05 was considered significant. All statistical analyses were performed with the IBM SPSS statistical software package (version 19.0; SPSS Inc, Chicago, IL).

The study was conducted according to the requirements of the institutional review board. The procedures of VH acquisition and periprocedural management were in agreement with the institutional guidelines.

Results

Fifty-six consecutive interventional therapies for cervical carotid artery stenosis in 52 patients were initially included in the present study. One patient with stenosis that was related to radiation therapy and one patient with restenosis after CEA were excluded from the study. Since the VH analyses of the plaque were not available, six stenotic lesions (three stenoses that were too severe for the VH IVUS catheter to cross before predilatation; three stenoses in which the raw RF data captured in the VH IVUS console could not be recorded on a digital video disc because of technical difficulties) were also excluded. The remaining 48 stenotic lesions in 45 patients were analyzed in this study. The descriptive characteristics are shown in Table 1.

The volumetric proportion of each plaque type (fibrous, fibrofatty, dense calcium, and necrotic core), and the proportion of the area of each plaque type at the minimum lumen site are given in Table 2.

The scattergraphs of the volumetric proportion of each plaque type against the proportion of the corresponding plaque type area at the minimum lumen site were drawn (Fig 1). Each regression line, the adjusted coefficient of determination, and its P value were also drawn in the graphs.

Discussion

In the present study, the authors analyzed the relationship between the volumetric composition of the entire carotid plaque and the plaque composition at the minimum lumen site using the simple regression analyses. The adjusted coefficients of determination of the simple regression analyses (Fig 1) were 0.782 for fibrous tissue, 0.741 for fibrofatty tissue, 0.864 for dense calcium, and 0.918 for necrotic core, which indicated a strong correlation. The volumetric proportion of each plaque type correlated significantly with the corresponding plaque type area at the minimum lumen site (Fig 1). This result gives support to the hypothesis that the plaque composition at the minimum lumen site represents the volumetric composition of the entire plaque that causes the stenosis.

The result of the present study is clinically useful for analyzing the relationships between the clinical prognosis of cervical carotid artery stenosis and carotid plaque composition. As described above, periprocedural hypotension in carotid artery stenting can be predicted by volumetric VH IVUS analysis of the plaque responsible for carotid artery stenosis.[23] While

volumetric analysis of the plaque is a time-consuming task,[13,14] analyzing only one cross-section at the minimum lumen site is easier and faster. The result of the present study enables easier prediction of periprocedural hypotension during CAS.

The factor most impeding plaque diagnosis with use of VH IVUS has been that analysis of the volumetric composition of the entire plaque responsible for the carotid artery stenosis is complex and time-consuming. The result of the present study, which enables easy analysis of carotid plaque, may contribute to the development of carotid plaque diagnosis with VH IVUS.[24,25]

Limitation of the Present Study

In the present study, the authors analyzed only atherosclerotic plaque in cervical carotid artery stenosis. Patients with stenosis related to radiation therapy or with restenoses after CEA were excluded from the present study. Further investigation is required for the analysis of these non-atherosclerotic plaques.

Conclusions

The result of the present study indicates that the plaque composition at the minimum lumen site represents the volumetric composition of the entire carotid plaque responsible for atherosclerotic cervical carotid artery stenosis.

Acknowledgments

The authors thank Dr. Tatsuo Takahashi, Dr. Shinichiro Tsugane, Dr. Noriyuki Susaki, Dr. Motoki Oheda, Dr. Toshiki Fukuoka, and Dr. Yosuke Tamari (Department of Neurosurgery, Nagoya Medical Center) for their helpful discussion.

Disclosure

The authors report no conflict of interest concerning the materials or methods used in this study or the findings specified in this paper.

References

1. Esposito L, Saam T, Heider P, Bockelbrink A, Pelisek J, Sepp D, Feurer R, Winkler C, Liebig T, Holzer K, Pauly O, Sadikovic S, Hemmer B, Poppert H. MRI plaque imaging reveals high-risk carotid plaques especially in diabetic patients irrespective of the degree of stenosis. BMC Med Imaging 2010;10:27.
2. Kurosaki Y, Yoshida K, Endo H, Chin M, Yamagata S. Association between carotid atherosclerosis plaque with high signal intensity on T1-weighted imaging and subsequent ipsilateral ischemic events. Neurosurgery 2011;68:62-67.
3. Yamada K, Yoshimura S, Kawasaki M, Enomoto Y, Asano T, Hara A, Minatoguchi S, Iwama T. Embolic complications after carotid artery stenting or carotid endarterectomy are associated with tissue characteristics of carotid plaques evaluated by magnetic resonance imaging. Atherosclerosis 2011;215:399-404.
4. Young VE, Patterson AJ, Sadat U, Bowden DJ, Graves MJ, Tang TY, Priest AN, Skepper JN, Kirkpatrick PJ, Gillard JH. Diffusion-weighted magnetic resonance imaging for the detection of lipid-rich necrotic core in carotid atheroma in vivo. Neuroradiology 2010;52:929-936.
5. Homburg PJ, Rozie S, van Gils MJ, van den Bouwhuijsen QJ, Niessen WJ, Dippel DW, van der Lugt A. Association between carotid artery plaque ulceration and plaque composition evaluated with multidetector CT angiography. Stroke 2011;42:367-372.
6. He C, Yang ZG, Chu ZG, Dong ZH, Shao H, Deng W, Chen J, Peng LQ, Tang SS, Xiao JH. Carotid and cerebrovascular disease in symptomatic patients with type 2 diabetes: assessment of prevalence and plaque morphology by dual-source computed tomography angiography. Cardiovasc Diabetol 2010;9:91.
7. Derlin T, Wisotzki C, Richter U, Apostolova I, Bannas P, Weber C, Mester J, Klutmann S. In vivo imaging of mineral deposition in carotid plaque using 18F-sodium fluoride PET/CT: correlation with atherogenic risk factors. J Nucl Med 2011;52:362-368.
8. Moustafa RR, Izquierdo Garcia D, Fryer TD, Graves MJ, Rudd JH, Gillard JH, Weissberg PL, Baron JC, Warburton EA. Carotid plaque inflammation is associated with cerebral microembolism in patients with recent transient ischemic attack or stroke: a pilot study. Circ Cardiovasc Imaging 2010;3:536-541.
9. Meyers PM, Schumacher HC, Gray WA, Fifi J, Gaudet JG, Heyer EJ, Chong JY. Intravascular ultrasound of symptomatic intracranial stenosis demonstrates atherosclerotic plaque with intraplaque hemorrhage: a case report. J Neuroimaging 2009;19:266-270.
10. Ravalli S, LiMandri G, Di Tullio MR, Marboe CC, Boxt L, Sacco RL, Schwartz A, Homma S. Intravascular ultrasound imaging of human cerebral arteries. J Neuroimaging 1996;6:71-75.
11. Nair A, Kuban BD, Tuzcu EM, Schoenhagen P, Nissen SE, Vince DG. Coronary plaque classification with intravascular ultrasound radiofrequency data analysis. Circulation 2002;106:2200-2206.
12. Nair A, Calvetti D, Vince DG. Regularized autoregressive analysis of intravascular ultrasound backscatter: improvement in spatial accuracy of tissue maps. IEEE Trans Ultrason Ferroelectr Freq Control 2004;51:420-431.
13. Nasu K, Tsuchikane E, Katoh O, Vince DG, Virmani R, Surmely JF, Murata A, Takeda Y, Ito T, Ehara M, Matsubara T, Terashima M, Suzuki T. Accuracy of in vivo coronary plaque morphology assessment: a validation study of in vivo virtual histology compared

with in vitro histopathology. J Am Coll Cardiol 2006;47:2405-2412.
14. Diethrich EB, Pauliina Margolis M, Reid DB, Burke A, Ramaiah V, Rodriguez Lopez JA, Wheatley G, Olsen D, Virmani R. Virtual Histology Intravascular Ultrasound Assessment of Carotid Artery Disease: The Carotid Artery Plaque Virtual Histology Evaluation (CAPITAL) Study. J Endovasc Ther 2007;14:676-686.
15. Rodriguez-Granillo GA, Vaina S, Garcia-Garcia HM, Valgimigli M, Duckers E, van Geuns RJ, Regar E, van der Giessen WJ, Bressers M, Goedhart D, Morel MA, de Feyter PJ, Serruys PW. Reproducibility of intravascular ultrasound radiofrequency data analysis: implications for the design of longitudinal studies. Int J Cardiovasc Imaging 2006;22:621-631.
16. Rodriguez-Granillo GA, Bruining N, Mc Fadden E, Ligthart JM, Aoki J, Regar E, de Feyter P, Serruys PW. Geometrical validation of intravascular ultrasound radiofrequency data analysis (Virtual Histology) acquired with a 30 MHz boston scientific corporation imaging catheter. Catheter Cardiovasc Interv 2005;66:514-518.
17. Rodriguez-Granillo GA, Serruys PW, Garcia-Garcia HM, Aoki J, Valgimigli M, van Mieghem CA, McFadden E, de Jaegere PP, de Feyter P. Coronary artery remodelling is related to plaque composition. Heart 2006;92:388-391.
18. Wehman JC, Holmes DR Jr, Ecker RD, Sauvageau E, Fahrbach J, Hanel RA, Hopkins LN. Intravascular ultrasound identification of intraluminal embolic plaque material during carotid angioplasty with stenting. Catheter Cardiovasc Interv 2006;68:853-857.
19. Takayama K, Taoka T, Nakagawa H, Myouchin K, Wada T, Sakamoto M, Fukusumi A, Iwasaki S, Kurokawa S, Kichikawa K. Successful percutaneous transluminal angioplasty and stenting for symptomatic intracranial vertebral artery stenosis using intravascular ultrasound virtual histology. Radiat Med 2007;25:243-246.
20. Tsurumi A, Tsurumi Y, Negoro M, Yokoyama K, Oheda M, Susaki N, Tsugane T, Takahashi T, Miyachi S. Subcutaneous Hematoma Associated with Manual Cervical Massage during Carotid Artery Stenting. A Case Report. Interv Neuroradiol 2011;17:386-390.
21. Irshad K, Millar S, Velu R, Reid AW, Diethrich EB, Reid DB. Virtual histology intravascular ultrasound in carotid interventions. J Endovasc Ther 2007;14:198-207.
22. Matsumoto S, Nakahara I, Higashi T, Iwamuro Y, Watanabe Y, Takezawa M, Murata D, Yokota T, Kira J, Yamada T. Fibro-fatty volume of culprit lesions in Virtual Histology intravascular ultrasound is associated with the amount of debris during carotid artery stenting. Cerebrovasc Dis 2010;29:468-475.
23. Tsurumi A, Miyachi S, Hososhima O, Izumi T, Ohshima T, Matsubara N, Kinkori T, Naito T, Wakabayashi T. Can periprocedural hypotension in carotid artery stenting be predicted? A carotid morphologic autonomic pathologic scoring model using virtual histology to anticipate hypotension. Interv Neuroradiol 2009;15:17-28.
24. Inglese L, Fantoni C, Sardana V. Can IVUS-virtual histology improve outcomes of percutaneous carotid treatment? J Cardiovasc Surg (Torino) 2009;50:735-744.
25. Schiro BJ, Wholey MH. The expanding indications for virtual histology intravascular ultrasound for plaque analysis prior to carotid stenting. J Cardiovasc Surg (Torino) 2008;49:729-736.

Table 1. Patient data and characteristics

Variables	Data	
Clinical characteristics		
Age (years)	68.8	(SD 7.1)
Female	6	(13%)
History		
Hypertension	33	(69%)
Diabetes mellitus	20	(42%)
Hyperlipidemia	28	(58%)
Coronary artery disease	15	(31%)
Congestive heart failure	4	(8%)
Lesion-related characteristics		
Lesion side: left	25	(52%)
Distance between carotid bifurcation and MLS ≤ 10 mm	36	(75%)
Distance between carotid bifurcation and MLS > 10 mm	12	(25%)
Plaque ulceration deeper than 2 mm	19	(40%)
Stenotic lesion involving both CCA & ICA	19	(40%)
Stenotic lesion involving only ICA	29	(60%)
Degree of stenosis (%)	73.6	(SD 15.3)
Contralateral ICA stenosis (> 50%) or occlusion	8	(17%)
Contralateral ICA occlusion	4	(8%)
Symptomatic carotid stenosis, ipsilateral	25	(52%)
Cerebral infarction, ipsilateral	18	(38%)
Cerebral infarction, contralateral	7	(15%)
Symptoms of carotid stenosis within 3 months, ipsilateral	11	(23%)
Cerebral infarction within 3 months, ipsilateral	7	(15%)
History of CAS or CEA, contralateral	5	(10%)

Continuous data are shown as the means (SD). Categorical data are shown as counts (%). SD = standard deviation; MLS = minimum lumen site; CCA = common carotid artery; ICA = internal carotid artery; CAS = carotid artery stenting; CEA = carotid endarterectomy.

Table 2. Virtual Histology Findings

Variables	Data	
Virtual Histology findings of plaque volumetric composition analysis		
Fibrous tissue (%)	61.0	(SD 12.8)
Fibrofatty tissue (%)	28.0	(SD 15.2)
Dense calcium (%)	3.9	(SD 6.2)
Necrotic core (%)	7.2	(SD 8.3)
Virtual Histology findings of plaque composition at MLS		
Fibrous tissue (%)	57.9	(SD 14.7)
Fibrofatty tissue (%)	31.6	(SD 16.8)
Dense calcium (%)	3.3	(SD 7.0)
Necrotic core (%)	7.1	(SD 9.5)

Data are shown as the means (SD). SD = standard deviation; MLS = minimum lumen site.

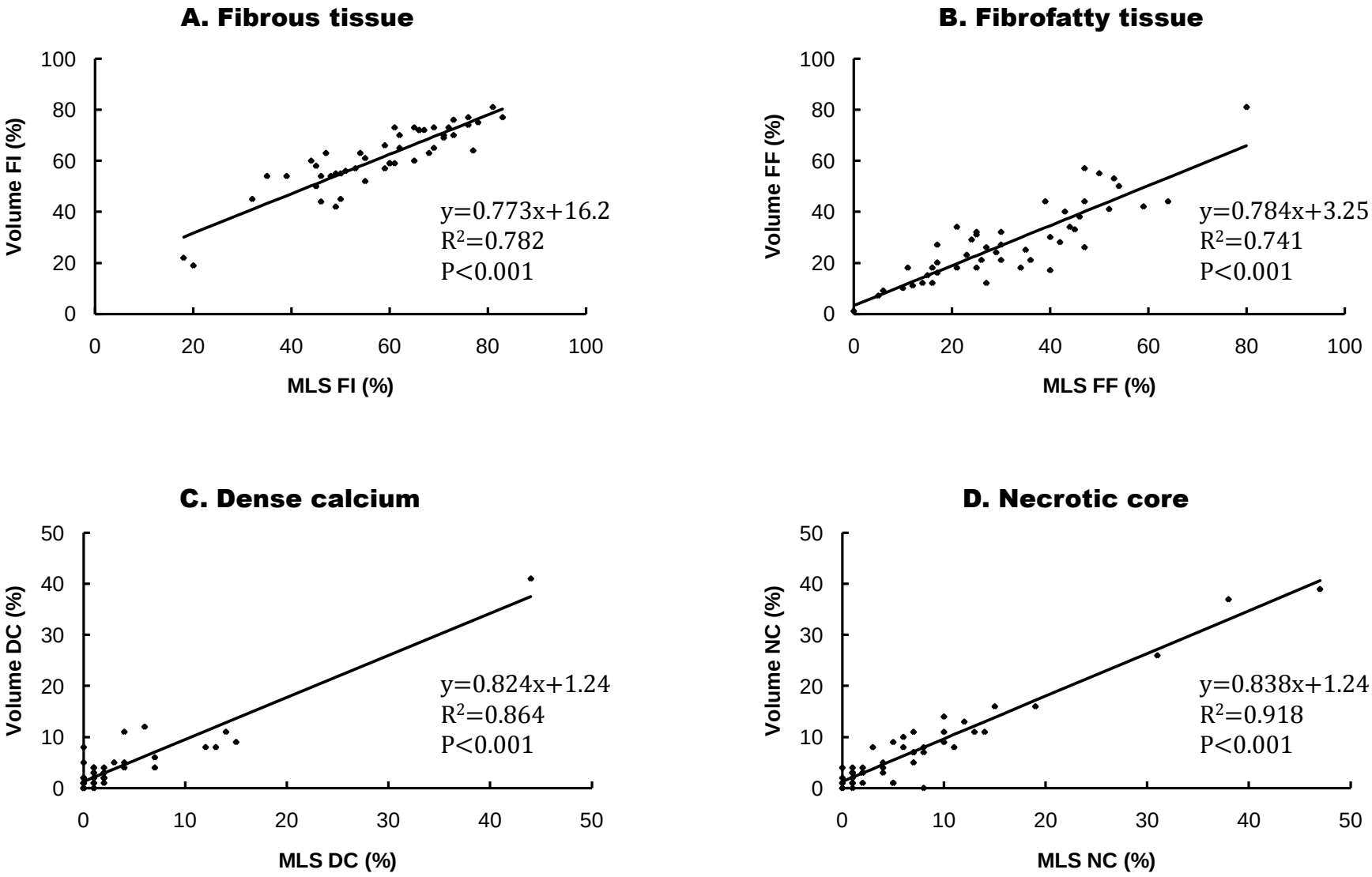
A. Fibrous tissue
Volume FI (%)
MLS FI (%)
y=0.773x+16.2
R²=0.782
P<0.001
B. Fibrofatty tissue
Volume FF (%)
MLS FF (%)
y=0.784x+3.25
R²=0.741
P<0.001
C. Dense calcium
Volume DC (%)
MLS DC (%)
y=0.824x+1.24
R²=0.864
P<0.001
D. Necrotic core
Volume NC (%)
MLS NC (%)
y=0.838x+1.24
R²=0.918
P<0.001

Fig 1. The scattergraphs and regression lines between the volumetric proportion of each plaque type (A. fibrous; B. fibrofatty; C. dense calcium; D. necrotic core) and the proportion of corresponding plaque type area at the minimum lumen site. FI = fibrous; FF = fibrofatty; DC = dense calcium; NC = necrotic core; MLS = minimum lumen site; R^2 = adjusted coefficient of determination.